ELSEVIER

Journal of Structural Geology 28 (2006) 834–849

JOURNAL OF STRUCTURAL GEOLOGY

www.elsevier.com/locate/jsg

Structural interplay between plutons during the construction of a batholith (Cerro Aspero batholith, Sierras de Córdoba, Argentina)

Lucio Pinotti [a,b], José M. Tubía [b,*], Fernando D'Eramo [a], Néstor Vegas [b], Ana M. Sato [c], Jorge Coniglio [a], Aitor Aranguren [b]

[a] *CONICET, Departamento de Geología, FCEFQyN, Universidad Nac. De Río Cuarto, P.O. Box 3, E-5800 Río Cuarto, Argentina*
[b] *Departamento de Geodinámica, Facultad de Ciencias, Universidad del País Vasco, P.O. Box 644, E-48080 Bilbao, Spain*
[c] *CONICET, Centro de Investigaciones Geológicas (CIG) Calle 1, 644, La Plata, Argentina*

Received 5 August 2005; received in revised form 8 February 2006; accepted 17 February 2006
Available online 31 March 2006

Abstract

Magnetic fabric patterns and microstructures of granitic rocks provide evidence of structural modifications as a result of the coalescence of two plutons, Alpa Corral and Talita, during the construction of a large granitic batholith, Cerro Aspero, in the Sierras Pampeanas of Córdoba (Argentina). The Alpa Corral granite is a small and nearly circular pluton, while the larger Talita pluton displays a marked N–S elongation. The NW quadrangle of the Alpa Corral pluton underwent a deformation resulting in foliation trajectories that outline a crescent moon pattern whose inner arc is concordant with the Alpa Corral/Talita contact. The highest values for the magnetic susceptibility and its anisotropy are concentrated in the coalescence zone between both plutons. The magmatic and sub-magmatic nature of the microstructures demonstrates that such a deformation was caused by the southward overriding of the largest Talita pluton while the Alpa Corral pluton was not yet fully crystallized. Rb–Sr geochronology indicates that this process took place 369 ± 9 Ma ago, long after the Famatinian (Ordovician to Early Devonian) deformation of the country rocks, which confirms a synmagmatic, rather than a regional, deformational event.

Keywords: Synmagmatic deformation; Pluton coalescence; Magnetic fabric; Sierras Pampeanas; Argentina

1. Introduction

In recent years, much of the motivation for understanding the processes of ascent and emplacement involved in the construction of granitic plutons has come from structural and geophysical approaches. Interpretations based on the bi-dimensional pictures unravelled by structural studies have been improved with the incorporation of gravity data that help to constrain the shape of the plutons at depth (Vigneresse, 1990; Aranguren et al., 1996; Améglio and Vigneresse, 1999). However, gravity surveys on granites are scarce and field-based structural studies of granitic intrusions are frequently restricted to plutons with well-defined planar fabrics, such as synkinematic plutons (Hutton, 1988; Hutton and Reavy, 1992; Archanjo et al., 1994b; Miller and Paterson, 2001) or porphyritic granites (Courrioux, 1987; Aranguren et al., 1996; Anma, 1997). In contrast, equigranular granites have been ignored, very often due to the fact that their lithological homogeneity and quasi-isotropic appearance make it virtually impossible for the naked eye to recognize the planar and linear structures. Such limitations can be overcome with the aid of the anisotropy of magnetic susceptibility, a geophysical tool capable of detecting subtle anisotropic fabrics, revealing that granite is always anisotropic (Bouchez, 1997; 2000). Whether they are field-based or magnetic-derived, structural interpretations of granites rely on the significance of their microstructures, an issue for which different solutions have been proposed (Guillet et al., 1983; Gapais and Barbarin, 1986; Blumenfeld and Bouchez, 1988; Paterson et al., 1998).

The construction of batholiths involves the growth and coalescence of plutons formed from magma injections through different feeder conduits. As a consequence, large parts of many batholiths consist of domains subjected to magmatic interactions between neighbouring intrusions. However, establishing the structural evolution on the basis of pluton coalescence is a difficult task. Structural patterns or microstructures that may be attributed to fabric overprinting in plutonic rocks are scarce and difficult to document.

* Corresponding author. Tel.: +34 946015392; fax: +34 946013500.
E-mail address: goptuxxj@lg.ehu.es (J.M. Tubía).

0191-8141/$ - see front matter © 2006 Elsevier Ltd. All rights reserved.
doi:10.1016/j.jsg.2006.02.004

Partially-melted rocks are very sensitive to the imprint of weak deformations (Benn, 1994), which can be associated either with emplacement-related flow or regional deformation. Probably for this very reason, despite the large data-set dealing with petrological or geochemical aspects of magmatic interactions (Stephens, 1992; Pitcher, 1993; Hecht and Vigneresse, 1999), only a few studies describe the structural evolution of collision zones between plutons (Gleizes et al., 1998).

This paper describes the origin of the distortion that overprinted the NW quadrangle of the Alpa Corral pluton when it coalesced with the larger Talita pluton to form the Devonian Cerro Aspero batholith of the Sierras de Cordoba, in Argentina (Fig. 1). The study combines structural and microstructural data with magnetic fabrics. Additional whole-rock Rb/Sr and muscovite K/Ar analyses of selected granite samples are included in order to more adequately constrain the age of the magmatism. The results of this study provide evidence that the deformation of the Alpa Corral pluton occurred under magmatic conditions, suggesting that large batches of incompletely crystallized magma may behave as non-Newtonian materials capable of transmitting compressional stresses.

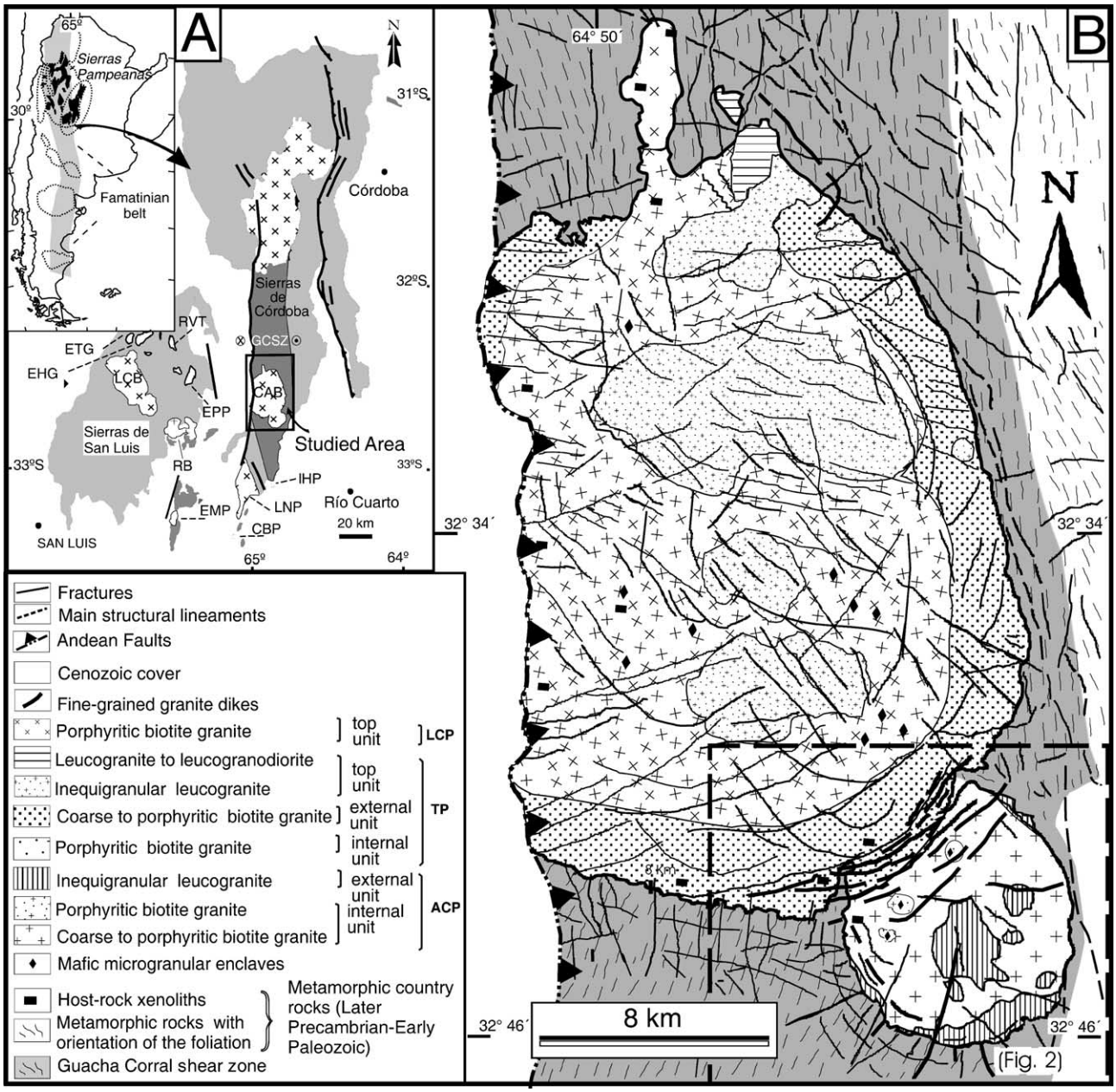

Fig. 1. (A) Geological map of the Sierras Pampenas de Córdoba and San Luis showing the Devonian batholiths with the location (insert) of the Cerro Aspero batholith. (B) Geological map of the Cerro Aspero batholith showing the petrographic zonation of the Alpa Corral (ACP), Talita (TP) and Los Cerros (LCP) plutons. The Cerro Aspero batholith intruded the Guacha Corral ductile shear zone. The western contact of the batholith is a reverse fault associated with the Cenozoic Andean tectonics of the Sierras Pampeanas.

2. Geological setting

The Cerro Aspero batholith is located in the Sierras de Córdoba, the easternmost part of the area known as Sierras Pampeanas, a system of N–S mountain ranges in western Argentina bounded by Neogene faults (Fig. 1A). The Sierras Pampeanas expose Precambrian to Paleozoic crystalline basement rocks of the Andes (Dalla Salda, 1987). The structural and metamorphic evolution of this basement reflects the overprinting of successive orogenic cycles (González Bonorino, 1950; Gordillo and Lencinas, 1979; Ortiz Suárez et al., 1992; Rapela et al., 1998a, 1999). The Late Precambrian–Cambrian Pampean Orogeny was replaced by the Famatinian Orogeny, dating from the Ordovician to the Late Devonian age. Paleozoic magmatism in the Sierras Pampeanas ended with the intrusion of a suite of batholiths between 380 and 360 m.y. (Stuart-Smith et al., 1999). Most of these Devonian batholiths display elongate shapes (Fig. 1A) and are composed of plutons that have discordant contacts with the country rocks and produce wide thermal aureoles. For these reasons, they are interpreted as post-tectonic intrusions (Ortiz Suárez et al., 1992; Pinotti et al., 2002; Sato et al., 2003). In the Sierras de Córdoba, the most penetrative foliation of the metamorphic rocks dips to the E and shows variable strikes to the N or NW. This regional foliation, currently referred to as S_3 (Martino et al., 1995), was reworked within regional-scale shear zones developed under amphibolite–greenschist-facies conditions during the closing stages of the Famatinian Orogeny (Martino

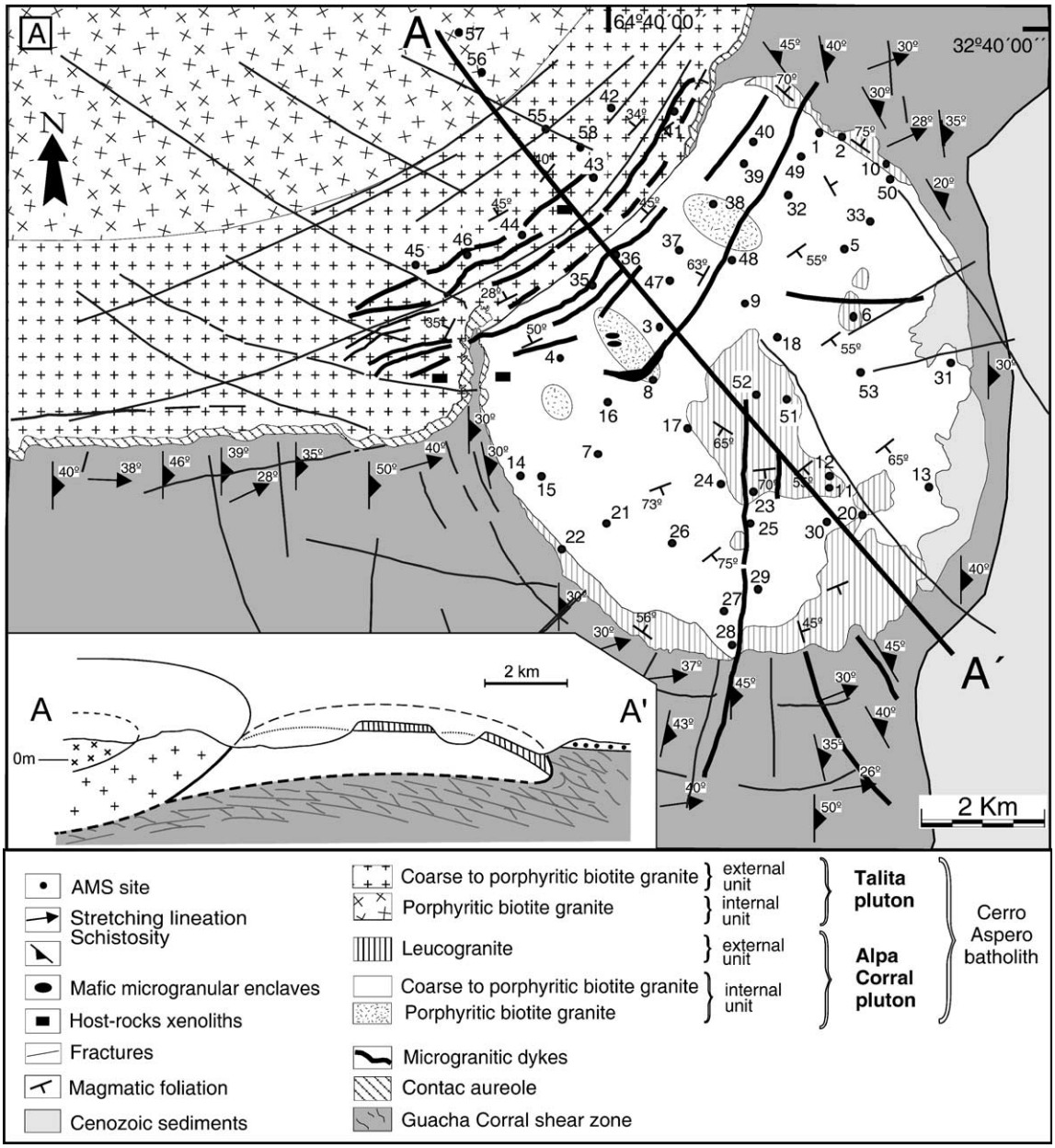

Fig. 2. (A) Geological and structural map of the Alpa Corral pluton and surrounding areas. Numbered dots indicate the location of the samples for the study of the magnetic fabric. (B) Cross-section showing the structural relationships between the Alpa Corral and Talita plutons.

et al., 1995; Rapela et al., 1998b). These N-trending and E-dipping shear zones consistently show top-to-the-W shear senses (Fig. 1B). The Cerro Aspero batholith intruded in one of these shear zones, named the Guacha Corral shear zone after Martino (1993, unpublished; referenced in Martino, 2003). With a thickness of 10–20 km and a length of more than 120 km (Fig. 1B), the Guacha Corral shear zone is a crustal-scale thrust that juxtaposed Cambrian and Ordovician rocks, with different metamorphic evolutions, during the Ordovician and Silurian (Martino et al., 1995; Fagiano et al., 2002; Martino, 2003). That the activity of the Guacha Corral shear zone predates the intrusion of the Cerro Aspero batholith is endorsed by the inclusion of mylonitic xenoliths in the Alpa Corral granite (Pinotti et al., 1997; Pinotti, 1998; Fagiano et al., 2002). The northward prolongation of the Guacha Corral shear zone is also referred to as the Tres Arboles shear zone (Whitmeyer and Simpson, 2003).

3. Field relationships and petrography of the Cerro Aspero batholith

The mylonites of the Guacha Corral shear zone are characterised by a consistent NNE-striking and E-dipping foliation (Fig. 2A). The contacts of the Cerro Aspero batholith with the Guacha Corral mylonites are sharp and steep dipping. However, as the Guacha Corral shear zone is truncated at a low

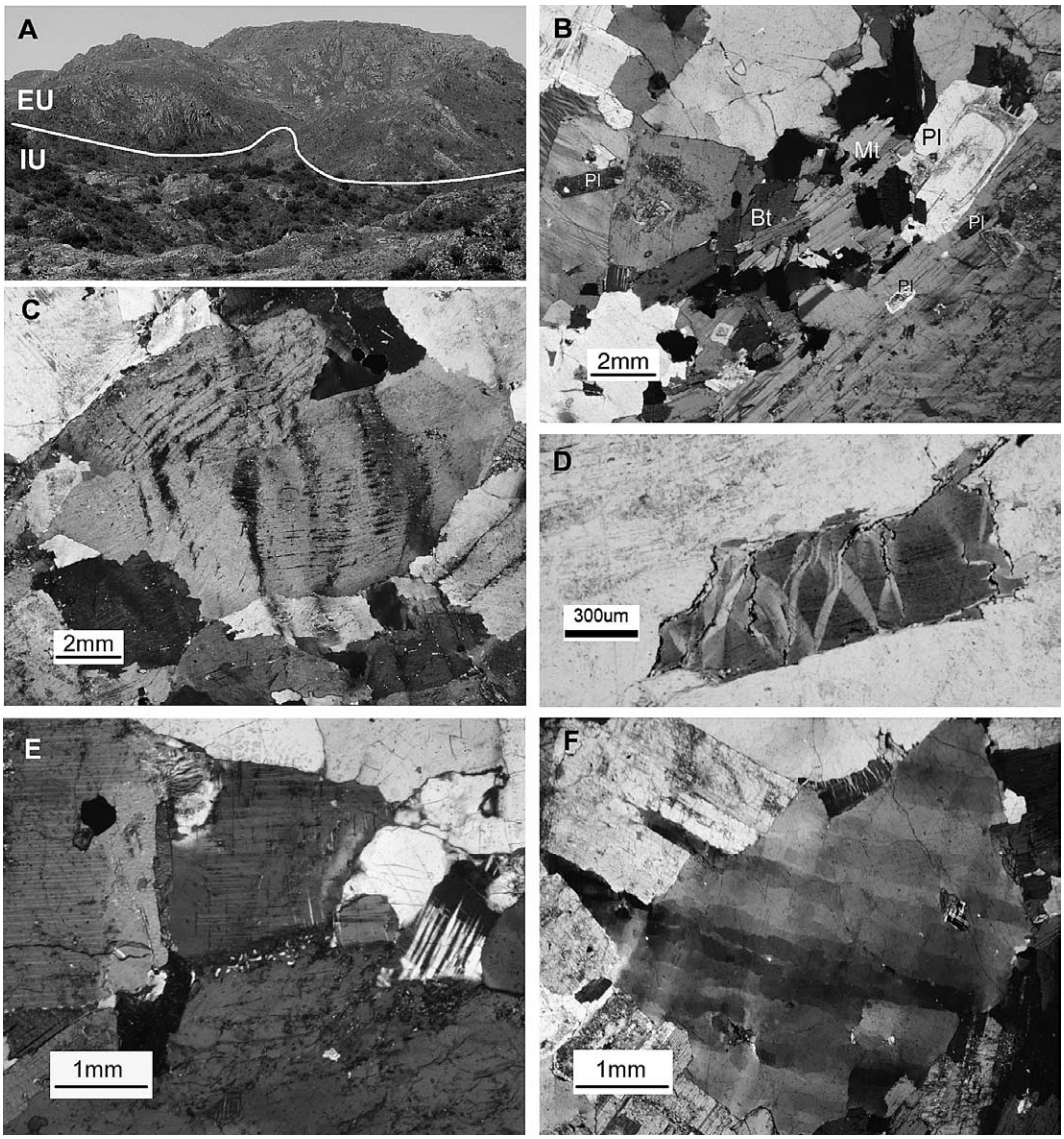

Fig. 3. Contact relationships and microstructures in the Alpa Corral pluton. (A) Large view of the central area of the pluton, showing the flat contact (white line) between the internal (IU) and external (EU) units. (B) Magmatic foliation drawn by the parallel arrangement of euhedral crystals of plagioclase (Pl) and elongate aggregates of biotite (Bt) coexisting with round aggregates of strain-free grains of quartz. Note that small grains of magnetite (Mt) also define this foliation. (C) Crystals of plagioclase showing microstructures of intracrystalline deformation by dislocation creep. (D) Conjugate kink bands in a crystal of biotite with inclusions of elongate magnetite grains (Mt) along the basal cleavage (001) of the host biotite; as such small grains of magnetite very often control the magnetic fabric of ferromagnetic granites, this type of microstructural observation supports the correlation of the magnetic fabric with the rock fabric. (E) Mechanical twins in a plagioclase crystal and K-feldspar with myrmekite rims, pointing to high-temperature deformation. (F) Sub-magmatic microfractures in K-feldspar intruded by wedges of quartz emanating from an equiaxial aggregate of quartz with mosaic microstructure.

Table 1
Rb–Sr and Sm–Nd analytical data

Sample no.	Field no.	Unit	Rb (ppm)	Sr (ppm)	$^{87}Rb/^{86}Sr$	Error	$^{87}Sr/^{86}Sr$	Error	ξSr (369)	$^{147}Sm/^{144}Nd$	$^{143}Nd/^{144}Nd$	TDM (Ma)	ξNd (369)
CIG-936	14.02.95.10	External	266.5	217.2	3.52908	0.07058	0.72488	0.00008	30.83				
CIG-937	M-78	Central	250.1	268.2	2.68471	0.05369	0.72093	0.00011	38.33	0.1097	0.512224	1441	−4.0
CIG-938	27.07.94	External	272.4	133.7	5.80572	0.11611	0.73830	0.00008	46.03	0.1228	0.512249	1451	−4.1
CIG-939	27.02.95.1	Central	257.5	224.9	3.33629	0.06672	0.72427	0.00012	39.88				
CIG-940	28.02.95.1	Central	285.8	198.2	4.28658	0.08573	0.72901	0.00008	42.98	0.1165	0.512236	1448	−4.1
CIG-941	27.07.94. LM	External	367.8	80.0	13.28379	0.26567	0.77671	0.00008	34.79				
CIG-942	M2	Central	181.9	473.0	1.13488	0.02269	0.71288	0.00008	42.23				
CIG-943	27.07.94.1	Dyke	294.3	38.7	22.80025	0.45600	0.82711	0.00010	90.44				

angle by the Talita pluton, the outline of the eastern contact of the batholith is nearly parallel to the mylonitic foliation. The western border of the Talita pluton is a reverse fault responsible for the westward thrusting of granites over Tertiary conglomerates (Fig. 1B), although Simpson et al. (2003) have suggested that this may be a Cretaceous normal fault.

The Alpa Corral pluton is a nearly circular (8 km in diameter) and concentrically zoned pluton that forms the southern part of the Cerro Aspero batholith (Fig. 2A). This pluton comprises a dominant, internal unit of biotite–granite and a minor, external unit made of leucogranite. The contact between these units is sharp and generally well exposed. The external unit is scattered in a marginal and steep-dipping ring sandwiched between the country rocks and the internal unit and a subhorizontal remnant, less than 50 m thick, located at the central part of the Alpa Corral pluton (Figs. 2A and 3A).

The biotite–granite of the internal unit shows large phenocrysts (5 cm) of perthitic microcline surrounded by a coarse-grained, granular groundmass integrated by plagioclase, biotite and quartz. Biotite usually forms elongate aggregates (Fig. 3B). Apatite, zircon and magnetite are accessory minerals. Magnetite can be observed as large crystals (> 1 mm) between the silicates of the groundmass (Fig. 3B) and as small inclusions, 5–120 μm long, parallel to the (001) cleavage of biotite. The grain size decreases and becomes more homogeneous in a peripheral band adjacent to the external unit. Biotite–schlieren and ovoid enclaves of fine-grained mafic minerals are common in the internal unit. The external unit is mainly composed of inequigranular, medium- to fine-grained leucogranite sheets that very often display chilled borders and are rich in miarolitic cavities and fluorite + molybdenite-bearing greisens. Such features point to crystallization from a residual magma enriched in volatile-fluids (Coniglio et al., 2000). The sub-horizontal structure of the central remnant is highlighted by the profuse intrusion of gently dipping aplitic sheets layered with beryl- and tourmaline-bearing pegmatitic lenses.

The Talita pluton expands over more than 385 km^2. It has three petrographic facies, referred to as internal, external and top units (Fig. 1B). The internal unit consists of pink, porphyritic, biotite–granite with abundant K-feldspar phenocrysts, up to 14 cm in length. Accessory minerals include titanite, allanite, magnetite, apatite and zircon. The external unit forms a roughly circular belt, 6–8 km wide, between the internal unit and the country rocks. It is made of pale-pink, coarse-grained, biotite granite with an equigranular texture. Finally, the top unit occurs as a discontinuous cap overlying the central and external units with sharp contacts. This unit consists of inequigranular leucogranite similar to that of the external unit of the Alpa Corral pluton.

4. Rb–Sr and K–Ar dating

Eight whole rock samples from the Alpa Corral pluton were selected to perform the Rb–Sr dating analysis. These consisted of four samples belonging to the internal unit, three to the external unit and the remaining one to a dyke. SiO_2 contents of

Table 2
K–Ar analytical data

Sample no.	Field no.	Mineral	Age (Ma)	^{40}Ar (scc/gr$\times10^{-5}$)	^{40}Ar (%)	K (%)
KA98-4882	ELTA	Moscovite	389±19	14.3	97.7	8.47
KA97-4637	MAC	Moscovite	379±18	13.9	97.6	8.44

the samples varied between 65 and 75%. Natural Sr was separated at the Centro de Investigaciones Geológicas (La Plata University), whereas quantitative FRX for total Rb and Sr, in addition to mass spectrometry analysis, were performed at the Centro de Pesquisas Geocronologicas (Sao Paulo University, Brazil). A single-collector VG354 mass spectrometer was used for the latter analysis. Additional Sm–Nd isotopic analyses were carried out at the Centro de Pesquisas Geocronologicas on three samples, using separated spiked Sm and Nd fractions that were analysed with a multi-collector Finnigan Mat 262 and the single-collector VG354 mass spectrometers, respectively. Concentrates of muscovite flakes from a sample of the external unit of the Alpa Corral pluton were analysed for the K–Ar relationship at Teledyne Brown Engineering, New Jersey (USA).

Tables 1 and 2 provide the obtained Rb–Sr, Sm–Nd and K–Ar analytical data. The samples analysed cover a wide range of ^{87}Rb/^{86}Sr between 1 and 23, with the highest values corresponding to the more differentiated external unit and to an aplitic dyke. Therefore, the isochrone obtained show a satisfactory data spread with an age of 369±9 Ma, initial ^{87}Rb/^{86}Sr=0.7069±0.0002 and MSWD=0.86 (Fig. 4). Since there is no evidence of structural reworking or metamorphism in the granite, we consider this to represent the crystallization age of the Alpa Corral pluton. Although the muscovite contains very high proportions of atmospheric ^{40}Ar, its K–Ar age, 379±18 Ma, is consistent, within the error limits, with the Rb/Sr age. Relatively low initial ^{87}Sr/^{86}Sr ratios between 0.704 and 0.707 are common in the granites from the Sierra de San Luis (Llambías et al., 1998), whereas in the Sierra de Córdoba, the Achala Batholith has ^{87}Sr/^{86}Sr ratios higher than 0.712 (Rapela et al., 1991).

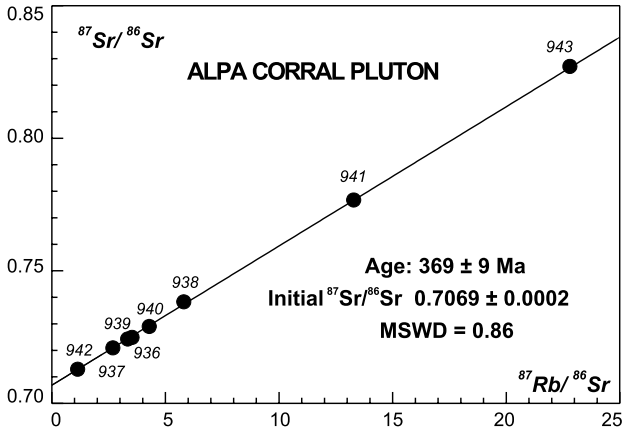

Fig. 4. Whole rock, Rb–Sr isochrone from the Alpa Corral pluton.

The T_{DM} depleted mantle model ages calculated from the Sm and Nd isotopic data are consistent, being between 1441 and 1448 Ma (after DePaolo et al., 1991), with $\xi Nd_{(369)}$ values between −4.0 and −4.1. The Meso-Proterozoic T_{DM} ages obtained for the Alpa Corral pluton coincide with the common Meso- to Paleo-Proterozoic time span indicated for Lower Paleozoic granites of the Sierras Pampeanas (Rapela et al., 1998b; Pankhurst et al., 1998, 2000). On the other hand, these T_{DM} model ages and the negative $\xi Nd_{(t)}$ values indicate derivation from a Meso-Proterozoic source enriched by crustal processes.

5. Structures in the Alpa Corral and Talita granites

The petrographic zoning of the Talita pluton and its contact with the Alpa Corral pluton are practically concordant (Fig. 2). The most evident structures of these plutons are the annular dykes that expand more than 7 km within the contact zone between the two plutons. These annular dykes propagate into the Alpa Corral pluton and the metamorphic host rocks (Fig. 2). The thickness of the dykes ranges from a few centimetres to 5 m and most of them are under 2 km in length.

Radial and annular fractures are frequent in the Alpa Corral granite. Some of these fractures spread more than 5 km through the country rocks (Fig. 2). The width of the annular fractures, which usually form en-échelon arrays, varies between 1 and 10 m. In contrast, many radial fractures are several kilometres long. Both the concentric and the radial fractures have irregular walls and display no evidence of shearing. This fracture network was used as channels for the intrusion of aplitic dykes. Steep-dipping fractures are widespread, even penetrative, within the central exposure of the external unit. Such fractures were also exploited by late hydrothermal fluids that percolated throughout the external unit, leading to advanced replacements of the magmatic minerals by secondary assemblages with chlorite, saussurite and oxides.

Microgranular mafic enclaves are common in the internal unit of the Alpa Corral pluton, but their spherical shape precludes their use as structural markers. Within the internal unit, the occasional presence of porphyritic textures facilitates the recognition of field foliations marked by the preferred orientation of K-feldspar megacrystals. Several microstructures point to the magmatic origin of this foliation, but there is also evidence of local overprints produced by a weak solid-state deformation that was active in sub-solidus to high temperature conditions (Fig. 3B–F). In general, the foliation is defined by the preferred orientation of strain-free, euhedral crystals of plagioclase and biotite coexisting with equiaxial aggregates of quartz without any microstructures of intracrystalline deformation (Fig. 3B). Microstructures supporting the action of solid-state deformation include bent crystals of plagioclase (Fig. 3C), kink bands in biotite (Fig. 3D) and mechanical twins in plagioclase (Fig. 3E). In the present case, these microstructures are accompanied by myrmekite rims at the borders of K-feldspar crystals (Fig. 3E) and aggregates of quartz with mosaic subgrains (Fig. 3F), which provide evidence of deformation at high temperature (Mainprice

et al., 1986; Simpson and Wintsch, 1989). The presence of feldspar porphyrocrystals with intracrystalline cracks filled with quartz containing mosaic subgrains (Fig. 3F) verifies that deformation started in sub-solidus temperature conditions, in accordance with the conditions required to develop sub-magmatic microfractures in granites (Bouchez et al., 1992). Furthermore, the mosaic microstructure in the grains of quartz suggests that the incipient deformation vanished at a high temperature, $>550\,^{\circ}C$, just after the crystallization of this mineral, as described by Mainprice et al. (1986) and Gapais and Barbarin (1986).

Microstructures resulting from the imprint of a weak solid-state deformation are more abundant within the external unit of the Talita pluton than in the Alpa Corral pluton. This is consistent with the elongation of mafic enclaves and the clearer expression of the foliation in this facies of the Talita pluton.

The foliation presents a dominant NE–SW strike in both plutons. This orientation, with regard to the Alpa Corral pluton, does not conform to its round shape, but to the contact with the Talita pluton (Fig. 2A). Microstructures pointing to solid-state deformation are concentrated close to the Talita pluton, in a NE-trending corridor that is partially segmented at high angles by several narrow domains characterised by the presence of a muscovite-bearing granite lacking deformation. Distant from contact with the Talita pluton, microstructures of magmatic origin are dominant, although a few NE bands of weakly deformed granite can still be found.

The cross-section of Fig. 2B shows the overriding of the Talita pluton across the Alpa Corral pluton by means of a NW-dipping contact. The shape of the Alpa Corral pluton at depth is speculative, as there is no gravity data for this region. Therefore, the laminar geometry and the thickness of this pluton have been calculated taking into account the empirical law of McCaffrey and Petford (1997). This law relates the length of granite intrusions to their thickness according to a scale invariant, power-law relationship.

6. Magnetic fabric of the Alpa Corral and Talita plutons

Two or three oriented cores were extracted with a portable drilling machine at 58 sites (positioned using a GPS with an accuracy of ± 10 m) over the Alpa Corral pluton and the southern part of the Talita pluton (Fig. 2A). Two hundred and seventy-six cylindrical samples (25 mm in diameter and 22 mm high) were obtained from these cores and their magnetic susceptibility was measured with a Kappabridge KLY-2 equipment, which works in a low alternating field (4×10^{-4} T; 920 Hz), with a resolution greater than 5×10^{-8} SI units.

6.1. Magnetic susceptibility data and magnetic mineralogy

The magnetic susceptibility of a rock, K, is defined as the ratio between its induced magnetization and the inducing magnetic field. For each sample, K was obtained as the arithmetic mean of the susceptibility values along the three axes, $(K_1+K_2+K_3)/3$, of the magnetic ellipsoid. The magnetic lineation (parallel to K_1) and foliation (normal to K_3) for each station were computed as the averages of the K_1 and K_3 orientations of the individual specimens. No less than one thin section per station was studied, with the aim of establishing the relationships between the magnetic fabric and the microstructures of the samples.

Table 3 summarizes the magnetic results. K values vary from 28 μSI to more than 17000 μSI, with averages of 1446 μSI for the internal unit and 134 μSI for the external unit. The distribution of K-values is bimodal and shows two maxima, which points to the coexistence of magnetite-poor ($K<300$ μSI) and magnetite-rich ($K>300$ μSI) areas in comparison with previous data from other granites (Rochette, 1987; Bouchez, 1997). The magnetic fabric of ferromagnetic plutons is mainly controlled by the high, intrinsic, magnetic susceptibility of ferromagnetic minerals such as magnetite, compared with paramagnetic granites, where K is mainly due to Fe-bearing silicates such as biotite or amphibole.

The variation of K with increasing temperature, from -193 to 700 °C, was analysed to identify the magnetic minerals responsible for the magnetic susceptibility, using a CS2-L apparatus and a CS-2 furnace coupled to the KLY-2. The recognition of the magnetic mineralogy of a rock is required in order to interpret the magnetic fabrics, particularly if the magnetic susceptibility is due to the contribution of different minerals with non-coaxial magnetic subfabrics (Rochette et al., 1992). As previously indicated, the low susceptibility values found in samples from the external unit of the Alpa Corral pluton (Table 3) suggest that their magnetic fabrics mainly reflect the contribution of paramagnetic minerals. However, the susceptibility versus temperature curve of a sample with low K (sample A6; Fig. 5) shows an increase in the susceptibility between 100 and 300 °C followed by a reduction in K at 370 °C, near the Curie temperature for maghemite. Neoformation of magnetite is evidenced by the higher value of K following the heating cycle and by the sudden increase in K after cooling below 590 °C, the Curie temperature for magnetite. Samples from the internal unit provide K-values ranging from 200 to 4000 μSI. The thermomagnetic curve of a sample from this unit (sample A11; Fig. 5) reveals the presence of magnetite, clearly shown by the K-maximum at -150 °C and the sudden fall in K at 590 °C, corresponding to the Vervey transition and the Curie temperature for magnetite, respectively. Nevertheless, a smaller T_c at 370 °C also suggests the presence of minor amounts of maghemite. Within the Talita samples, the K values range from 8000 to 20000 μSI, which is consistent with the observation of abundant magnetite crystals in thin sections. The presence of this mineral is also demonstrated by thermomagnetic curves characterized by well-defined Vervey and Curie transitions (samples A42 and A43; Fig. 5). The heating curve of the A42 specimen shows that K increases from 150 °C up to 350 °C and decreases at 430 °C. These features imply the existence of a magnetic phase that is transformed during the heating path. The heating curve is not reversible and the cooling path to room

temperature conditions records higher values of K and the production of new magnetite. Similar results have been attributed to the neoformation of magnetite from unstable Ti-bearing maghemite during the heating of samples from room temperature to 700 °C (Kontny and Dietl, 2002).

6.2. Magnetic fabric: directional and scalar data

Fig. 6 presents the orientation of magnetic foliations and lineations. In the external unit of the Talita pluton, the strike of the foliation and the trend of the lineation are adapted to

Table 3
AMS data for 58 sampling stations (three samples have been excluded as they provide non-interpretable results) of the Alpa Corral (internal, Int, and external, Ext, facies) and Talita (TP) plutons. K: magnetic susceptibility, in μSI; P': anisotropy degree; T: shape parameter; K_1: azimuth and plunge of the magnetic lineation; K_3: azimuth and plunge of the magnetic foliation pole

Site	Unit	K	K_1	K_3	P'	T
A1	Int	1177	182/30	352/57	1.126	−0.51
A2	Ext	80	125/64	307/19	1.045	−0.25
A3	Int	819	339/53	102/20	1.044	0.05
A4	Int	320	236/85	94/4	1.058	−0.71
A5	Int	1530	009/37	210/52	1.188	−0.80
A6	Ext	201	190/78	300/8	1.045	0.16
A7	Int	844	349/76	123/3	1.085	0.05
A8	Int	474	270/31	75/57	1.079	−0.56
A9	Int	3286	86/35	357/3	1.063	0.30
A10	Ext	38	348/25	105/38	1.047	0.30
A11	Int	3237	100/29	343/29	1.119	0.38
A12	Ext	164	186/38	357/52	1.034	0.04
A13	Int	1251	58/20	316/11	1.069	0.01
A14	Ext	28	242/66	96/10	1.025	−0.42
A15	Int	522	127/66	340/17	1.068	0.34
A16	Int	1061	218/27	350/62	1.113	0.40
A17	Int	2624	77/47	334/14	1.095	−0.25
A18	Int	1510	191/64	339/5	1.105	0.11
A20	Int	847	113/55	323/24	1.085	−0.18
A21	Int	494	158/60	316/27	1.041	−0.06
A23	Ext	31	331/23	202/55	1.051	0.72
A24	Int	2344	218/37	110/29	1.086	−0.08
A25	Int	2254	227/37	100/34	1.043	0.11
A26	Int	2154	204/50	282/15	1.045	0.09
A27	Int	3247	–	–	1.101	−0.16
A28	Ext	100	110/71	354/18	1.013	−0.07
A29	Int	2150	226/11	327/39	1.091	0.26
A30	Int	3716	224/59	315/3	1.057	−0.34
A31	Int	1394	149/60	19/16	1.056	−0.35
A32	Int	889	320/77	123/8	1.102	−0.04
A33	Int	1810	237/86	327/4	1.114	0.69
A35	Int	17133	358/53	163/36	1.162	0.57
A36	Int	14568	237/6	142/53	1.205	0.09
A37	Int	14318	257/26	151/29	1.141	0.33
A38	Int	84.7	283/7	199/32	1.118	0.47
A39	Int	56	009/51	164/37	1.044	0.34
A40	Int	1683	67/76	173/11	1.214	−0.13
A41	TP	12357	008/57	189/33	1.240	−0.49
A42	TP	9310	26/7	165/76	1.139	−0.26
A43	TP	16268	217/18	351/63	1.187	−0.12
A44	TP	11763	237/14	124/43	1.113	0.09
A45	TP	7826	273/70	138/19	1.096	0.10
A46	TP	14926	248/6	001/48	1.155	−0.14
A47	Int	1266	221/2	125/42	1.093	0.60
A48	Int	422	121/33	25/13	1.093	0.08
A49	Int	397	38/50	135/15	1.086	0.34
A50	Int	1044	55/46	246/44	1.051	−0.15
A51	Ext	446	350/81	128/6	1.055	−0.32
A52	Ext	71	235/18	141/13	1.033	0.40
A53	Int	1030	31/27	150/36	1.102	0.17
A54	Int	1798	127/44	272/40	1.091	0.14
A55	TP	15888	26/12	136/64	1.101	0.20
A56	TP	6508	243/40	117/42	1.114	0.32
A57	TP	8768	258/63	131/14	1.241	0.54
A58	PT	8189	226/13	315/24	1.204	−0.10

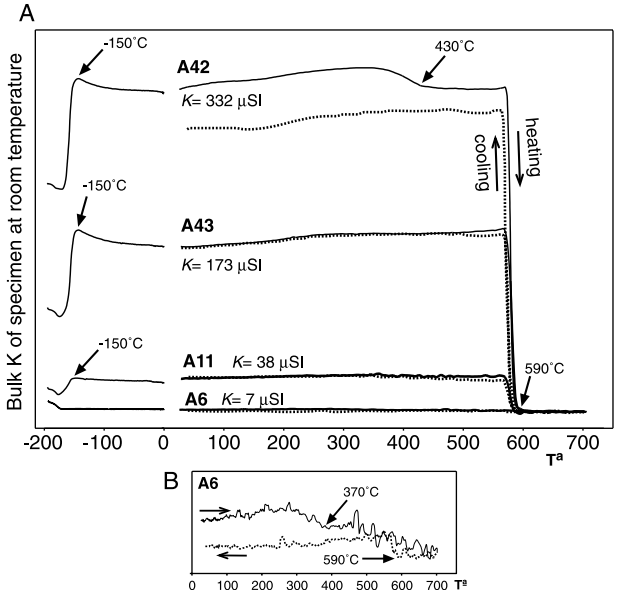

Fig. 5. Thermomagnetic curves illustrating the variation of K-values as a function of the temperature. The magnetic susceptibility values have not been normalized to the volume of powder and, therefore, are much lower than those of the solid core specimen. The inset (B) shows an extended view of the heating and cooling curves of the sample A6. See the text for a detailed explanation of the figures.

the contact convexity with the Alpa Corral pluton (Fig. 6A). NW-dipping foliations reveal that the Talita granite rests on the Alpa Corral pluton. The dominant low-plunging lineations of the external unit of the Talita pluton contrast with the steep-dipping lineations found in its internal unit (Fig. 6B). Based on interpretations of displacement paths of magma (Paterson et al., 1998; see their fig. 2B), such a change could be interpreted in terms of divergent flow within the outer part of the pluton related to magma inflow from the NW to the SE.

Within the Alpa Corral pluton the magnetic foliations do not outline a circular pattern, but there is a dominant NE–SW striking and steeply dipping foliation (Fig. 6A: stereoplot). A rough NE–SW boundary can be traced between a western domain with dominant NW-dipping foliations and an eastern domain with SE-dipping foliations. This boundary is parallel to the Talita/Alpa Corral contact, as are most of the magnetic foliations. In contrast, magmatic foliations in the internal unit of the Alpa Corral pluton are at high angles to the flat contact with the central exposure of the external unit (Fig. 6A). We consider these relationships to indicate that: (1) the foliation of the internal unit postdates the development of the magmatic zoning, and (2) the formation of the foliation was strongly influenced by the SW-spreading of the overriding Talita pluton. It is worth noting that within the porphyritic granites a satisfactory correlation exists between the magnetic foliation of the measured samples and the magmatic foliations observed in the field (compare Figs. 2 and 6). This may be due to the fact that the magnetic fabric mainly reflects the orientation of weakly elongated magnetite inclusions in biotite. As previously pointed out, the inclusions of magnetite are parallel to the (001) cleavage of biotite (Fig. 3B) and, in turn, biotite is concordant with the foliation defined in the field by the K-feldspar fenocrystals. The magnetic lineation displays very variable trends, but high plunges (Fig. 6B).

Within the central hills of the external unit (Alpa Corral pluton), the magnetic foliation rests at a high angle to the weakly dipping magmatic layering (Fig. 6A). In this area, the magnetic fabric no longer reflects structures of magmatic origin, but the orientation of succeeding vertical joints. The concordance between the magnetic fabric and these fractures explains the variable and weak values for the magnetic susceptibility, $K < 300$ μSI, obtained for all of the measured samples from the external unit. Mainly because these fractures—and the related microcracks observed in orientated thin sections—are enriched in aggregates of iron hydroxides that were formed by hydrothermal alteration.

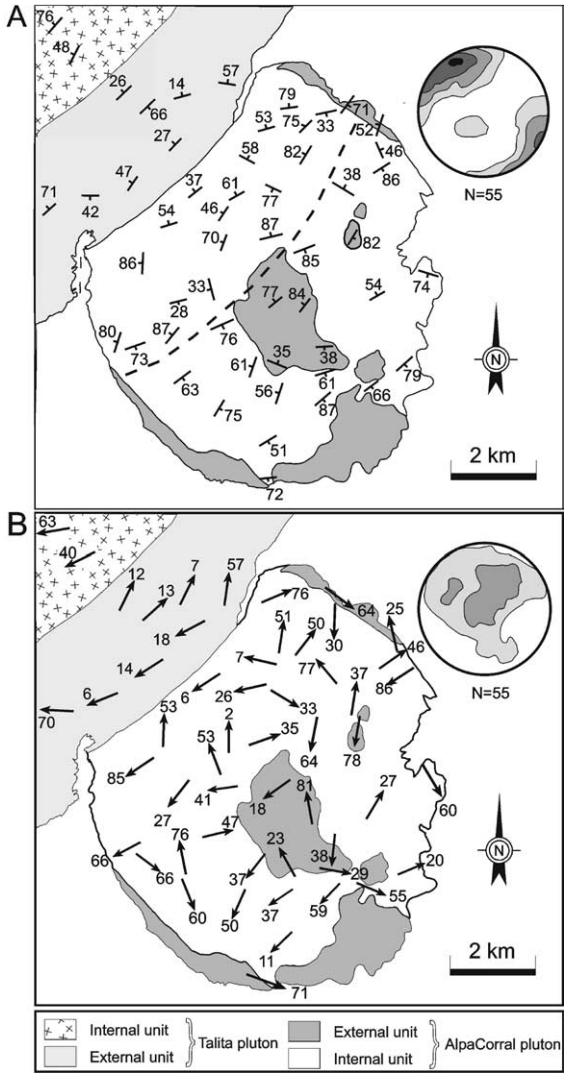

Fig. 6. Structural maps showing the magnetic foliation (A) and lineation (B) in the Alpa Corral pluton and the southern part of the Talita pluton. In (A), the curved line within the Alpa Corral pluton virtually outlines the boundary between a northern domain with NW-dipping foliations and a southern domain with dominant SE-dipping foliation. The stereoplots provide the orientation of the poles towards the foliation (A) and the lineation (B); equal-area net, lower hemisphere projection, intervals: 1, 2, 3, etc., times uniform distribution.

The anisotropy degree (P') ranges from 1.013 to 1.2401 (Table 3), with 42% of the sites having $P'>1.10$. It is interesting to observe that most (69.5%) of the samples with $P'>1.10$ come from the Talita pluton and the NW domain of the Alpa Corral pluton. This fact provides an additional argument supporting the enhancement of the magmatic foliation in the colliding zone between the two plutons. As is frequently observed in granites, there is neither correlation between P' and K (Table 3) nor between Jelinek's (1981) shape parameter, T, of the magnetic ellipsoids and their anisotropy degree, P' (Table 3).

6.3. ARM

In order to obtain the preferred orientation of the magnetic grains, the anisotropy of remanent magnetization (ARM) was studied using the partial anhysteretic remanence anisotropy method (pAAR) (Trindade et al., 2001). This procedure consists of cycles of anhysteretic remanence acquisition, measurement and demagnetization along different positions for each sample. A six-position measurement scheme was used, which corresponds to three mutually orthogonal positions directed in two opposite senses. The differences between the supposed identical data are considered in order to design the confidence zone of each axis.

Measurements of the partial anhysteretic remanence anisotropy were performed based on remanent coercivity spectra (Fig. 8). The 2–20 mT (pAAR2–20) and 5–30 mT (pAAR5–30) windows were chosen to analyse the range of low coercivities; the main one was used to consider the magnetic anisotropy of samples with large-sized magnetite grains. Coercivity values under 2 mT were removed in order to avoid the effects of viscous remanences. The upper limit of the window, 20 mT, was set to avoid any disturbance from the possible presence of small-sized magnetite related to different subfabrics. In sample A6, from the magnetite-poor external unit, the selected window has been changed to 5–30 mT, thereby adjusting it to the main remanence peak of its coercivity spectrum. In all but the A52 sample, following normalization and subtraction of the viscous remanences, the intensities of the low coercivity windows correspond to over 70% of the total measured remanence.

The magnetic fabrics for the low coercivity windows are represented in Fig. 7. The main result is the coincidence between the AMS fabrics and the pAAR2–20 fabrics for the samples with a high magnetite content from El Talita pluton and the Internal Unit of the Alpa Corral granite. In these rocks, we can consider the AMS fabric to be coaxial with the magnetite shape fabric (Grégoire et al., 1995) which, in turn, will be coaxial with the crystalline fabric of the rock (Archanjo et al., 1994b). Conversely, magnetite-poor samples from the external unit present different fabric patterns that are in agreement with the AMS fabrics, but are affected by their weak magnetic anisotropies and small magnetization values. The former effect can produce axis inversion (A6 sample), whereas the latter can increase the probability of the error spreading (A52 sample).

6.4. Coercivity spectra and hysteresis loops

The study of the magnetic phases has been complemented by coercivity spectra and hysteresis measurements (Figs. 8 and 9). Remanent coercivity spectra were determined by deriving the curve values taken from the magnetization of the sample, applying a small steady field (500 μT DC field) superposed to an alternating magnetic field (AF) of 100 mT, and their subsequent gradual demagnetization, by an alternating field. In order to conduct this we have used an LDA3–AMU1 demagnetizer–anhysteretic magnetizer and a JR5A magnetometer supplied by Agico (Brno). This procedure was applied to eight samples representative of the Alpa Corral and Talita plutons.

Fig. 8 shows the spectra obtained, with unimodal distributions typical of low-coercivity grains. In the case of the internal unit of the Alpa Corral (sample A11) and the external unit of the Talita pluton (samples A42 and A43), the predominant magnetic phase is magnetite. From this, we can conclude that these samples contain large magnetite grains in

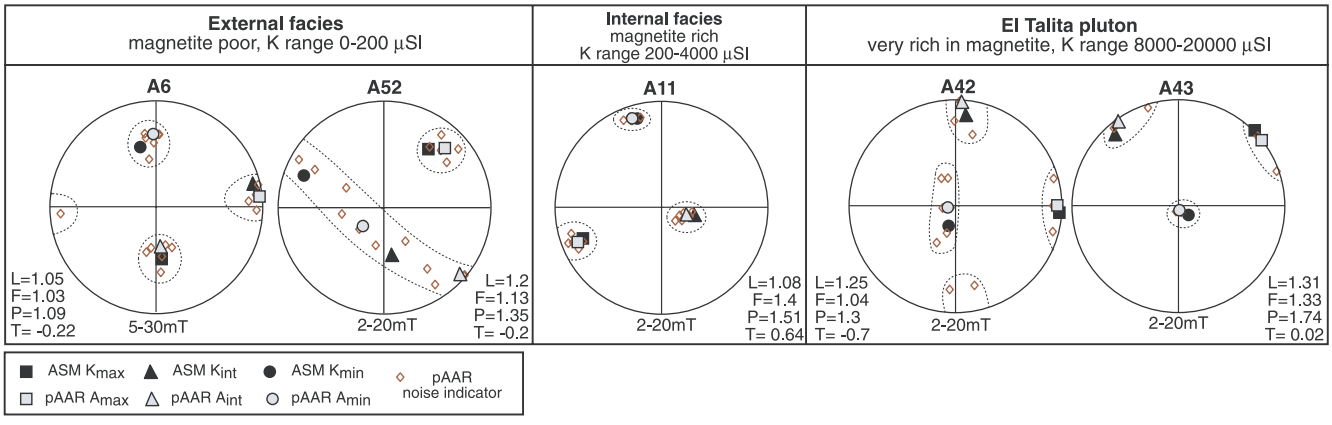

Fig. 7. Partial anisotropy of anhysteretic remanent (pAAR) in the windows 2–20 and 5–30 mT, for the three igneous facies. The measured AMS axes of each sample are marked by black symbols (K_{max}: square, K_{int}: triangle, K_{min}: circle) and the equivalent axes of the analysed coercivity windows are shown in grey. The diamond symbols represent the noise indicators related to each component. Anisotropy parameters for the studied sites are included. L: linear anisotropy (A_{max}/A_{int}); F: planar anisotropy (A_{int}/A_{min}); P: anisotropy degree (A_{max}/A_{min}); T: Jelinek's (1981) shape parameter $=(\ln F-\ln L)/(\ln F+\ln L)$.

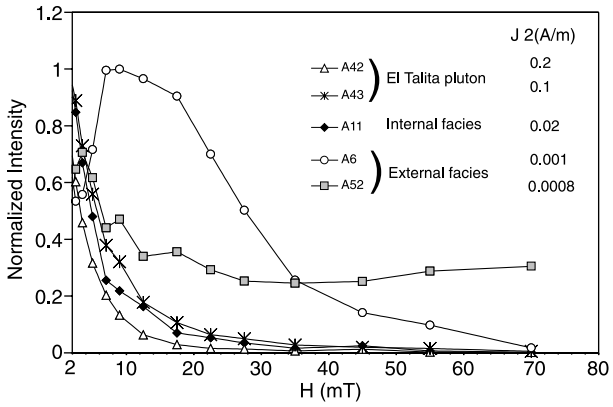

Fig. 8. Remanent coercivity spectra derived from tumbling AF demagnetization of a 100 mT anhysteretic remanence (DC field of 0.05 mT). Intensities of remanence are normalized to the highest value of partial remanent acquisition. *J* 2(A/m) are the measured values of remanent intensity at 2 A/m for each sample.

a multi-domain state, since coercivities in magnetite are linked to grain sizes (Jackson et al., 1988; Jackson, 1991). The samples from the external unit of the Alpa Corral pluton (A6 and A52) reflect very small intensity values and provide different spectra. Sample A6 reflects a bimodal distribution of coercivities with a main peak for the lowest ones, whereas sample A52 is more complex with low coercivities composed by many peaks and an increasing background remanence at the end part of the spectra. This background remanence is related to the presence of hematite.

Hysteresis loops have been measured, up to ± 1 Tesla at room temperature, in samples with the highest and lowest ferromagnetic contents. In both cases, the hysteresis loops are narrow-waisted, a typical feature of ferromagnetic grains with low-coercivity (Fig. 9). The Mrs/Ms and Hcr/Hc hysteresis ratios (Mrs: remanence magnetization after saturation; Ms: saturation magnetization; Hcr: coercivity of remanence; Hc: coercivity) from sample A43 fall into the multi-domain field (MD) of the Day's diagram (Day et al., 1977). Subsequently, a minimum grain size >10 μm can be estimated for such MD-magnetite. The sample from the external unit (A52) shows a complex hysteresis loop where total saturation is reached in two stages, pointing to the existence of two ferromagnetic phases. The hematite deduced from the coercivity spectra would be responsible for the second saturation stage. In addition, the shape of this curve reveals the importance of the paramagnetic minerals in this external unit.

7. Discussion

7.1. Was the emplacement of the Cerro Aspero batholith shear-zone controlled?

Many emplacement studies of granites, from a variety of geological settings and crustal levels, conclude that there is a causative link between synkinematic plutons and ductile shear zones (Hutton, 1988; Hutton and Reavy, 1992; Archanjo et al., 1994a; Weinberg et al., 2004). However, some synkinematic granites do not fulfil this relationship (Paterson and Schmidt, 1999). First, the weak obliquity between the NNW–SSE elongation of the Cerro Aspero batholith and the N–S strike of the Guacha Corral shear zone (Fig. 1) suggests that the emplacement of this batholith was shear-zone controlled. However, the age of the Alpa Corral pluton and the current appreciation of the regional geology do not support such an interpretation. The 369 ± 9 Ma age obtained from Rb–Sr analysis constrains the age of emplacement of the Alpa Corral pluton. Within the error limits, this age is consistent with previous U–Pb ages reported in other post-tectonic granites of the Sierras de Córdoba, for example the Achala batholith (368 ± 2 Ma; Dorais et al., 1997) or the Los Nogales Granite (382 ± 6 Ma; Stuart-Smith et al., 1999). These Late Devonian ages allow us to discard any direct link between the emplacement of the Cerro Aspero batholith and the formation of the older, Ordovician–Silurian, Guacha Corral shear zone. At the regional scale, other large batholiths in the Sierras Pampeanas, like that of Las Chacras (Fig. 1A), display N–S to NNW–SSE elongate geometries on a map, but are unrelated to any outcropping shear zone.

Previous works in the Sierras de San Luis (Brogioni, 1992; López de Luchi et al., 2002) propose that the emplacement of intrusions similar to the Cerro Aspero batholith was associated with an extensional event. According to such interpretations, it could be argued that the crustal thickening of the Famatinian Orogen from Middle Ordovician to Early Devonian times (Martino, 2003; Sato et al., 2003; Simpson et al., 2003) may

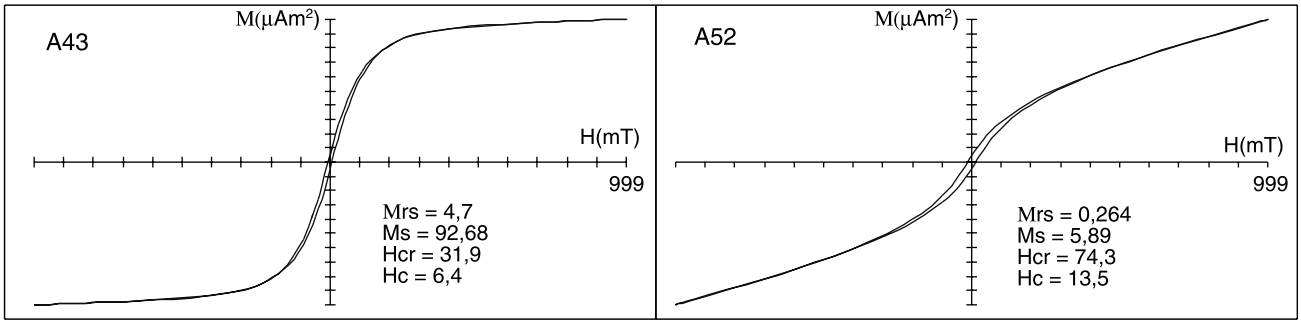

Fig. 9. Representative hysteresis loops for the El Talita and the Alpa Corral external facies (M: magnetization; H: applied field). The loops are not corrected for paramagnetic slopes and the hysteresis parameters are included (Mrs: saturation remanence magnetization; Ms: saturation magnetization; Hcr: remanent coercive force; Hc: coercive force).

have given way to extensional collapse from Early Devonian times onwards. However, this interpretation is not consistent with the tectonic data hitherto compiled for this region, which reveal that most of the reported crustal-scale shear zones display reverse or strike-slip motions, pointing to compressional conditions (Martino, 2003). For this present case, we suggest that local extensional conditions in an overall convergent setting, such as tension fractures at high angles to shear zones, could have triggered favourable conditions for the ascent of magma, as previously demonstrated by gravity studies on granites emplaced in compressional settings (Aranguren et al., 1996, 1997).

7.2. Deformation induced by collision of plutons.

In the following model, we assemble structural and magnetic data (Fig. 10), in an attempt to explain the origin and evolution of the distortion in the NW quadrangle of

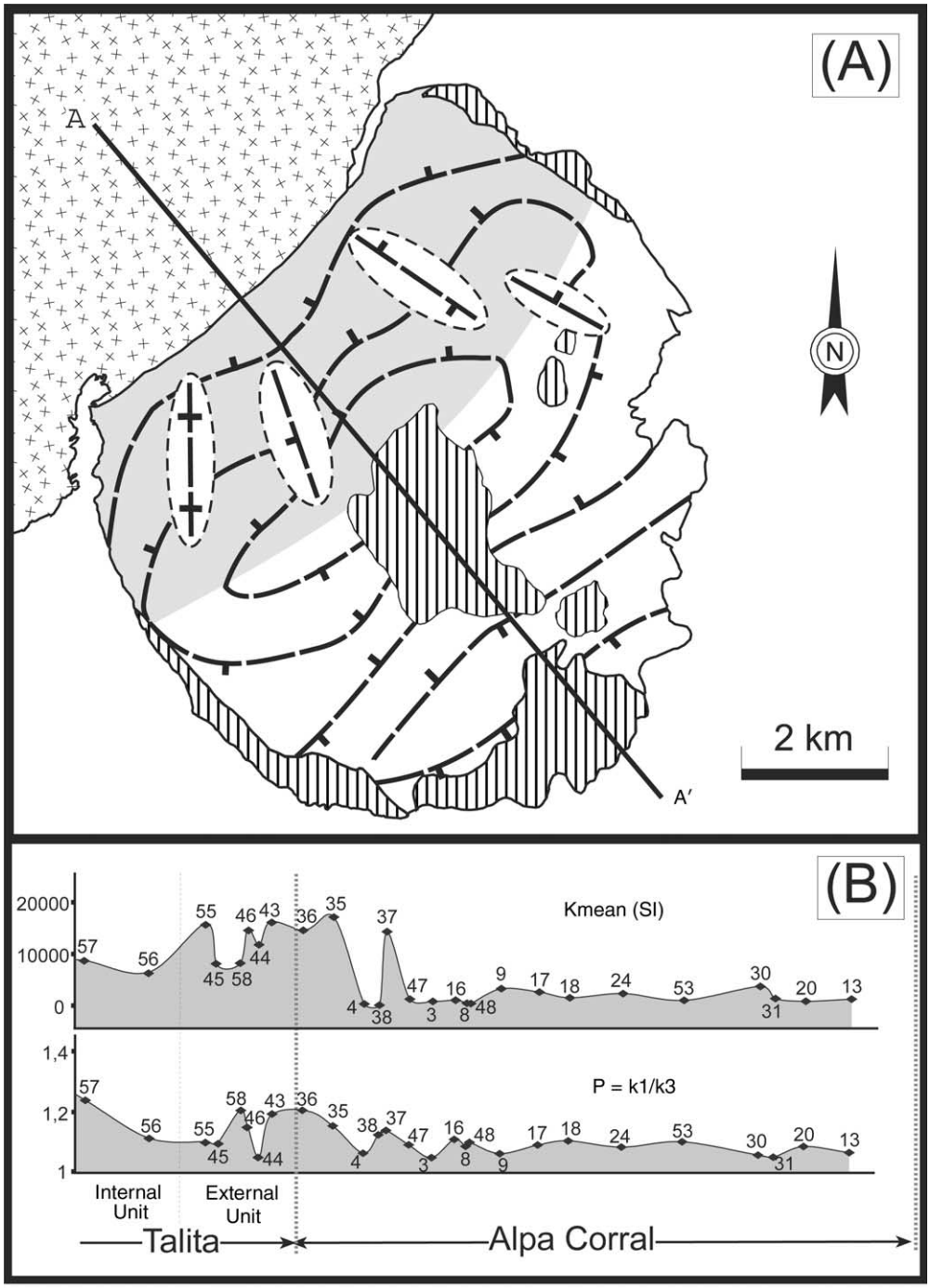

Fig. 10. (A) Map of foliation trajectories in the Alpa Corral pluton. The foliation trajectories outline an elongate antiform parallel to the contact with the Talita pluton. The NW-limb of the antiform coincides with the sector (grey pattern) where, in high-temperature conditions, sub-solidus deformation is concentrated. This limb is disrupted at a high angle by several areas formed by strain-free granite. (B) Variation of *K*- and *P*-values along a transect across the Alpa Corral/Talita contact.

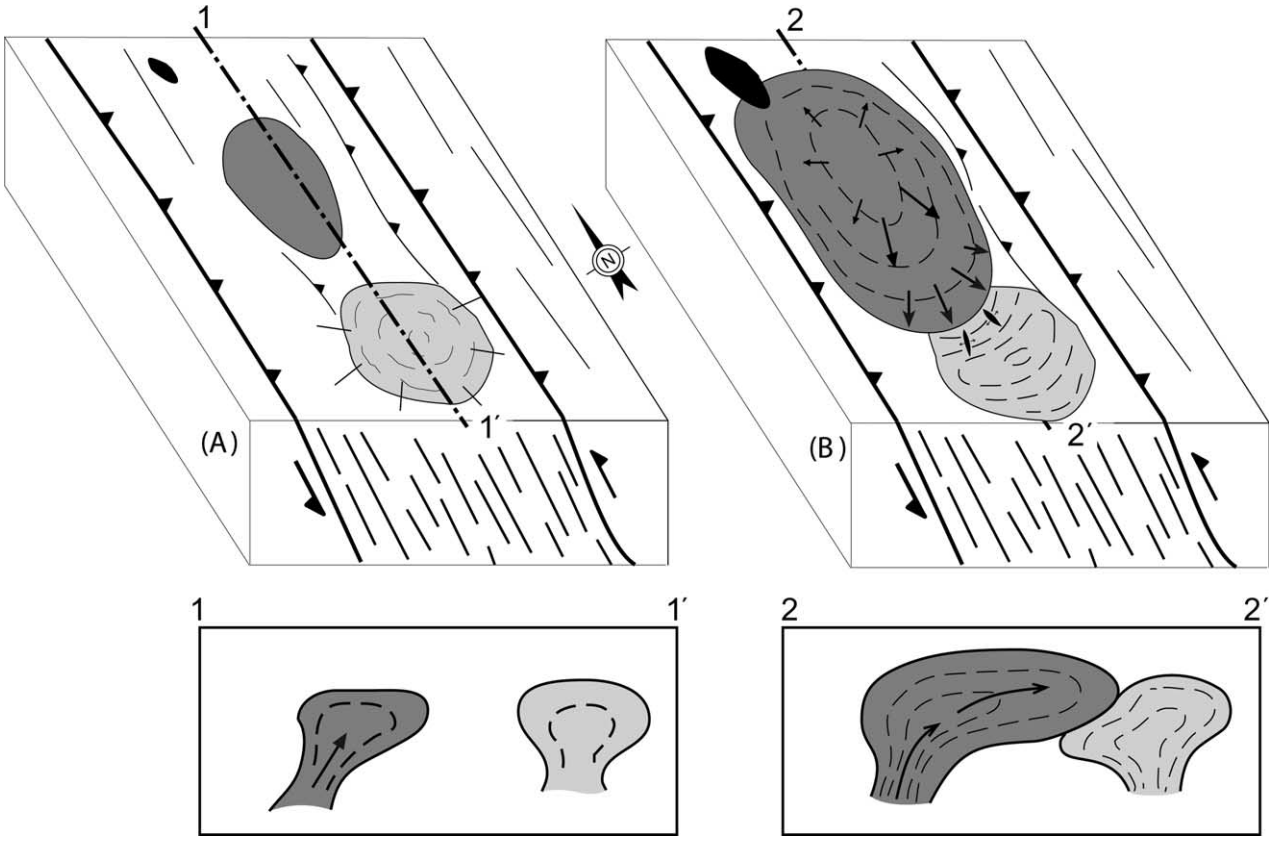

Fig. 11. Sequence of magmatic pulses implicated in the formation of the Cerro Aspero batholith. (A) Incipient magmatic stage with the Alpa Corral and Talita bodies evolving as isolated intrusions. (B) Southward expansion of the Talita pluton, ending in collision with the Alpa Corral pluton. The strain field established in the coalescence zone produced the distortion of the NW-quadrangle of the Alpa Corral pluton.

the Alpa Corral pluton (Fig. 11). Foliation trajectories outline a crescent-moon pattern, corresponding to an asymmetric antiform with NE–SW elongation and a curved hinge line, which is roughly parallel to the Alpa Corral/Talita contact (Fig. 10A). Microstructures indicative of sub-solidus or solid-state deformation at high-temperature are mainly concentrated in the northwestern limb of such an antiform. It is worth noting, however, that the NW limb is disrupted by NW–SE elongated domains, formed by granites devoid of sub-solidus or solid-state deformation microstructures and displaying foliations at high angles to the foliation trajectories. On the whole, these strain-free domains outline a fan converging towards the Talita pluton (Fig. 10A), similar to potential radial fractures associated with the Talita pluton. In general, *K*- and *P*-values also increase towards the contact between the two plutons (Fig. 10B). In our opinion, these structural features are consistent with the overprinting of pre-existing magmatic fabrics of the Alpa Corral pluton by the deformation induced by the overriding of the Talita pluton.

The concordance between the AMS and the pAAR2–20 fabrics indicates the coaxiality of the AMS fabrics with the shape of magnetite crystals, which leads to the correlation between magnetic fabrics and field foliations (Fig. 3B). Based upon microstructural observations that point to the magmatic origin of the foliation (Fig. 3), we consider that the magnetic fabric provides a frozen image of the late stages of magma deformation. This is a relevant point when explaining the formation of the concave outline of the northwestern contact of the Alpa Corral pluton, since many foliations of this granite are subparallel to such contact (Figs. 6A and 10A). These features suggest that pre-existing planar fabrics of the Alpa Corral pluton experienced additional flattening to accommodate the southward spreading of the Talita pluton. The lack of the external unit of Alpa Corral during the contact with the Talita pluton also supports the previous interpretation, owing to the fact that the overlap by huge volumes of hot magma could prevent the fast cooling of the outer shell of the Alpa Corral pluton and/or promote its mechanical erosion.

Fig. 11 represents the evolution proposed in order to explain the distortion of the Alpa Corral pluton. At an early stage, two independent magmatic bodies started to spread laterally from different feeding channels (Fig. 11A). The two incipient bodies are focalized within the pre-existing Guacha Corral shear zone. This may be due to the fact that large-scale shear zones behave as domains of crustal weakness, which are frequently reactivated during subsequent orogenic cycles (Butler et al., 1997), thus triggering the opening of fractures through which magma ascend. At this stage, the Alpa Corral pluton would display a circular shape and concentric magmatic fabrics.

McNulty et al. (2000) described the coalescence of several magma batches with different compositions to form a large pluton. The construction of the Cerro Aspero batholith

involved two main magma batches with similar compositions that competed between themselves for the space. However, as they started to grow at different times, the rheological behaviour of such magma batches was different when they coalesced (Pinotti et al., 2002).

Due to the growth and southward expansion of the Talita body, the two plutons coalesced and a local strain field was established on both sides of the collision zone (Fig. 11B). According to the sub-solidus to high temperature deformation observed in the zone of convergence of these two plutons, this second stage occurred while both plutons were still partly molten, probably with a smaller melt fraction in the Alpa Corral body. Since only a small strain overprint is required to reorient the lineation in partly crystallized magmas (Benn, 1994), different crystallization percentages would explain that lineations in the external unit of the Talita pluton are parallel to the contact of the plutons, while lineations in the NW-quadrangle of the Alpa Corral pluton are characterized by a noticeable dispersion (Fig. 6B). As a hypothesis, we propose that the local strain field was also responsible for the formation of the domains with strain-free granite transecting the NW-limb of the antiform defined by the foliation trajectories (Fig. 10A), as this would be affected by compression leading to the compaction of the overall limb and melt extraction towards local dilation bands (Fig. 11B). This is a well-established mechanism for melt extraction within high-grade metamorphic rocks suffering partial melting (Brown, 2004). We are aware that there are significant rheological differences between the lower continental crust and a partially molten body. However, we suggest that this process could work in magmatic systems with melt fractions close to the second rheological threshold and which behave as a non-Newtonian to Bingham body. If our interpretation is correct, the NW-limb of the Alpa Corral pluton could represent the field expression of the entire domain bounded by the first and second rheological thresholds of Arzi-type diagrams.

8. Conclusions

Magnetic fabric patterns and microstructures of granitic rocks provide evidence of structural modifications due to the coalescence of the Alpa Corral and Talita plutons during the construction of the Cerro Aspero batholith, in the Sierras Pampeanas of Córdoba (Argentina). The growth of the Talita pluton was mainly accomplished by the lateral inflow of magma from the NNE to the SSW. The southward expansion of this pluton induced a strain field within the NW-quadrangle of the Alpa Corral pluton. The foliation trajectories resulting from this process outline a crescent moon pattern whose inner arc is concordant with the Alpa Corral/Talita contact. This strain field was active while the Alpa Corral pluton was not yet fully crystallized and behaved as a non-Newtonian to Bingham body. Rb–Sr geochronological data indicate that this process occurred at 369 ± 9 Ma ago, long after the Ordovician deformation of the country rocks, which is in line with a magmatic, rather than a regional, deformational event.

Acknowledgements

The authors wish to thank the CONICET and the Departamento de Geología (UNRC, Argentina) for the logistical support. This work was financed by grant 18/C162 (SECYT, UNRC, Argentina) and research projects CGL2004-00701/BTE (Ministerio de Educación y Ciencia, Spain) and 9/UPV00001.310-14478/2002 (Grupos Consolidados, Universidad del País Vasco, Spain). The helpful comments made by Eugenio Aragón and Eduardo Llambías and the revision of a former manuscript by F. Hongn and A.S. Yoshinobu are greatly appreciated.

References

Améglio, L., Vigneresse, J.L., 1999. Geophysical imaging of the shape of granitic intrusions at depth: a review. In: Castro, A., Fernández, C., Vigneresse, J.L. (Eds.), Understanding Granites: Integrating New and Classical Techniques. Geological Society of London, Special Publications 168, pp. 39–54.

Anma, R., 1997. Oblique diapirism in the Yakushima granite in the Ryukyu arc, Japan. In: Bouchez, J.L., Hutton, D.H.W., Stephens, W.E. (Eds.), Granite: From Segregation of Melt to Emplacement Fabrics. Kluwer, Dordrecht, pp. 287–311.

Aranguren, A., Tubía, J.M., Bouchez, J.L., Vigneresse, J.L., 1996. The Guitiriz granite, Variscan belt of northern Spain: extension-controlled emplacement of magma during tectonic escape. Earth and Planetary Science Letters 139, 165–176.

Aranguren, A., Larrea, F.J., Carracedo, M., Cuevas, J., Tubía, J.M., 1997. The Los Pedroches batholith (southern Spain): polyphase interplay between shear zones in transtension and setting of granites. In: Bouchez, J.L., Hutton, D.H.W., Stephens, W.E. (Eds.), Granite: From Segregation of Melt to Emplacement Fabrics. Kluwer, Dordrecht, pp. 215–229.

Archanjo, C.J., Bouchez, J.L., Corsini, M., Vauchez, A., 1994a. The Pombal granite pluton: magnetic fabric, emplacement and relationships with the Brasiliano strike-slip setting of NE Brazil (Parabai State). Journal of Structural Geology 16, 323–335.

Archanjo, C.J., Launeau, P., Bouchez, J.L., 1994b. Magnetic fabrics vs. magnetite and biotite shape fabrics of the magnetite-bearing granite pluton of Gameleiras (Northeast Brazil). Physics of the Earth and Planetary Interiors 89, 63–75.

Benn, K., 1994. Overprinting of magnetic fabrics in granites by small strains: numerical modelling. Tectonophysics 233, 153–162.

Blumenfeld, P., Bouchez, J.L., 1988. Shear criteria in granite and migmatite deformed in the magmatic and solid states. Journal of Structural Geology 10, 361–372.

Bouchez, J.L., 1997. Granite is never isotropic: an introduction to ASM studies of granitic rocks. In: Bouchez, J.L., Hutton, D.H.W., Stephens, W.E. (Eds.), Granite: From Segregation of Melt to Emplacement Fabrics. Kluwer, Dordrecht, pp. 95–112.

Bouchez, J.L., 2000. Anisotropie de susceptibilité magnétique et fabrique des granites. C.R. Acad. Sci. Paris, Sciences de la Terre et des planètes 330, 1–14.

Bouchez, J.L., Delas, C., Gleizes, G., Nédélec, A., Cuney, M., 1992. Submagmatic microfractures in granites. Geology 20, 35–38.

Brogioni, N., 1992. Geología del batolito de Las Chacras–Piedras Coloradas, Provincia de San Luis. Revista del Museo de la Plata, Nueva Serie, Sección Geología 11, 1–16.

Brown, M., 2004. The mechanism of melt extraction from lower continental crust of orogens. In: Ishihara, S., Stephens, W.E., Harley, S.L., Arima, M., Nakajima, T. (Eds.), Fifth Hutton Symposium. The Origin of Granites and Related Rocks. The Geological Society of America. Special Paper 389, pp. 35–48.

Butler, R.W., Holdsworth, R.E., Lloyd, G.E., 1997. The role of basement reactivation in continental deformation. Journal of the Geological Society, London 154, 69–71.

Coniglio, J., Xavier, R.P., Pinotti, L., D'Eramo, F., 2000. Ore-forming fluids of vein-type fluorite deposits of the Cerro Aspero batholith, Southern Córdoba Province, Argentina. International Geology Review 42, 368–383.

Courrioux, G., 1987. Oblique diapirism: the Criffel granodiorite/granite zoned pluton (southwest Scotland). Journal of Structural Geology 3, 313–330.

Dalla Salda, L., 1987. Basement tectonic of the Southern Pampean Ranges. Tectonics 6, 249–260.

Day, R., Fuller, M., Schmidt, V.A., 1977. Hysteresis properties of titanomagnetites: grain-size and compositional dependence. Physics of the Earth and Planetary Interiors 13, 260–267.

DePaolo, D.J., Linn, A.M., Schubert, G., 1991. The continental crustal age distribution: methods of determining mantle separation ages from Sm–Nd isotopic data and application to the southwestern United States. Journal of Geophysical Research 96, 2071–2088.

Dorais, M.J., Lira, R., Chen, Y., Tingey, D., 1997. Origin of biotite–apatite-rich enclaves, Achala batholith, Argentina. Contributions to Mineralogy and Petrology 130, 31–46.

Fagiano, M., Pinotti, L., Esparza, A.M., Martino, R., 2002. La faja de cizalla Guacha Corral, Sierras Pampeanas de Córdoba, Argentina. 15° Congreso Geológico Argentino, Actas 1, pp. 259–264.

Gapais, D., Barbarin, B., 1986. Quartz fabric transition in a cooling syntectonic granite (Hermitage massif, France). Tectonophysics 125, 357–370.

Gleizes, G., Leblanc, D., Santana, V., Olivier, P., Bouchez, J.L., 1998. Sigmoidal structures featuring dextral shear during emplacement of the Hercynian granite complex of Cauterets–Panticosa (Pyrenees). Journal of Structural Geology 20, 1229–1245.

González Bonorino, F., 1950. Algunos problemas geológicos de las Sierras Pampeanas. Revista de la Asociación Geológica Argentina 5, 81–110.

Gordillo, C., Lencinas, A., 1979. Sierras Pampeanas de Córdoba y San Luis. Segundo Simposio de Geología Regional Argentina, Academia Nacional de Ciencias, Córdoba 1, 577–650.

Grégoire, V., Saint Blanquat, M., Nédélec, A., Bouchez, J.L., 1995. Shape anisotropy versus magnetic interactions of magnetite grains: experiments and application to AMS in granitic rocks. Geophysical Research Letters 22, 2765–2768.

Guillet, P., Bouchez, J.L., Wagner, J.J., 1983. Anisotropy of magnetic susceptibility and magnetic structures in the Guérande granite massif (France). Tectonics 2, 419–429.

Hecht, L., Vigneresse, J.L., 1999. A multidisciplinary approach combining geochemical, gravity and structural data: implications for pluton emplacement and zonation. In: Castro, A., Fernández, C., Vigneresse, J.L. (Eds.), Understanding Granites: Integrating New and Classical Techniques. Geological Society of London, Special Publication 168, pp. 95–110.

Hutton, D.H.W., 1988. Granite emplacement mechanisms and tectonic controls: inferences from deformation studies. Transactions of the Royal Society of Edinburgh: Earth Sciences 79, 245–255.

Hutton, D.H.W., Reavy, R.J., 1992. Strike-slip tectonics and granite petrogenesis. Tectonics 11, 960–967.

Jackson, M., 1991. Anisotropy of magnetic remanence: a brief review of mineralogical sources, physical origins, and geological applications and comparison with susceptibility anisotropy. Pure and Applied Geophysics 136, 1–28.

Jackson, M., Gruber, W., Marvin, J., Banerjee, S.K., 1988. Partial anhysteretic remanence and its anisotropy: applications and grain-size dependence. Geophysical Research Letters 15, 440–443.

Jelinek, V., 1981. Characterization of the magnetic fabric of rocks. Tectonophysics 79, 63–70.

Kontny, A., Dietl, C., 2002. Relationships between contact metamorphism and magnetite formation and destruction in a pluton's aureole, White–Inyo Range, eastern California. Geological Society of America Bulletin 114, 1438–1451.

Llambías, E.J., Sato, A.M., Ortiz Suárez, A., Prozzi, C., 1998. The granitoids of the Sierra de San Luis. In: Pankhurst, R., Rapela, C. (Eds.), The Proto-Andean Margin of Gondwana. Geological Society of London Special Publications 142, pp. 325–341.

López de Luchi, M.G., Rapalini, A.E., Rosello, E., Geuna, S., 2002. Rock and magnetic fabric of the Renca Batholith (Sierra de San Luis, Argentina): constraints on emplacement. Lithos 61, 161–186.

Mainprice, D., Bouchez, J.L., Blumenfeld, P., Tubía, J.M., 1986. Dominant c-slip in naturally deformed quartz: implications for dramatic plastic softening at high temperatures. Geology 14, 819–822.

Martino, R., 2003. Las fajas de deformación dúctil de las Sierras Pampeanas de Córdoba: Una reseña general. Revista de la Asociación Geológica Argentina 58, 549–571.

Martino, R., Kramer, P., Escayola, M., Giambastiani, M., Arnosio, M., 1995. Transecta de las Sierras Pampeanas de Córdoba a los 32° S. Revista de la Asociación Geológica Argentina 50, 60–77.

McCaffrey, K.J., Petford, N., 1997. Are granitic intrusions scale invariant? Journal of the Geological Society, London 154, 1–4.

McNulty, B.A., Tobisch, O.T., Cruden, A.R., Gilder, S., 2000. Multistage emplacement of the Mount Givens pluton, central Sierra Nevada batholith, California. Geological Society of America Bulletin 112, 119–135.

Miller, R.B., Paterson, S.R., 2001. Construction of mid-crustal sheeted plutons: examples from the North Cascades, Washington. Geological Society of America Bulletin 113, 1423–1442.

Ortiz Suárez, O.A., Prozzi, C., Llambías, E.J., 1992. Geología de la parte sur de la Sierra de San Luis y granitoides asociados. Revista Estudios Geológicos 48, 269–277.

Pankhurst, R.J., Rapela, C.W., Saavedra, J., Baldo, E., Dahlquist, J., Pascua, I., Fanning, C.M., 1998. The Famatinian magmatic arc in the central Sierras Pampeanas: an Early to Mid-Ordovician continental arc on the Gondwana margin. In: Pankhurst, R., Rapela, C. (Eds.), The Proto-Andean Margin of Gondwana. Geological Society of London, Special Publications 142, pp. 343–367.

Pankhurst, R.J., Rapela, C.W., Fanning, C.M., 2000. Age and origin of coeval TTG, I- and S-type granites in the Famatinian belt of NW Argentina. Transactions of the Royal Society of Edinburgh: Earth Sciences 91, 151–168.

Paterson, S.R., Schmidt, K.L., 1999. Is there a close spatial relationship between faults and plutons? Journal of Structural Geology 21, 1131–1142.

Paterson, S.R., Fowler, T.K., Schmith, K.L., Yoshinobu, A.S., Yuan, E.S., Miller, R.B., 1998. Interpreting magmatic fabric patterns in plutons. Lithos 44, 53–82.

Pinotti, L.P., 1998. El batolito Cerro Áspero, Provincia de Córdoba. Modelo de intrusión y su relación con la evolución de las Sierras Pampeanas. Ph.D. Thesis, Universidad Nacional de Río Cuarto.

Pinotti, L.P., Llambías E.J., Coniglio, J., 1997. Stoping as a main mechanism of intrusion in post-tectonic granite from the southern part of the Sierra de Comechingones, Sierras Pampeanas de Córdoba, Argentina. Second International Symposium on Granites and Associated Mineralizations, Salvador, Bahia, Brazil. Abstracts with Programs, pp. 323–325.

Pinotti, L., Coniglio, J., Esparza, A., D'Eramo, F., Llambías, E., 2002. Nearly circular plutons emplaced by stoping at shallow crustal levels, Cerro Aspero Batholith, Sierras Pampeanas de Córdoba, Argentina. Journal of South American Earth Sciences 15, 251–265.

Pitcher, W.S., 1993. The Nature and Origin of Granite. Chapman and Hall, London.

Rapela, C.W., Pankhurst, R.J., Kirschbaum, A., Baldo, E.G.A., 1991. Facies intrusivas de edad carbonífera en el batolito de Achala: evidencia de una anatexis regional en las Sierras Pampeanas. 6° Congreso Geológico Chileno, Viña del Mar. Actas 1, pp. 40–43.

Rapela, C.W., Pankhurst, R.J., Casquet, C., Baldo, E., Saavedra, J., Galindo, C., 1998a. Early evolution of the proto-andean margin of South America. Geology 26, 707–710.

Rapela, C.W., Pankhurst, R.J., Casquet, C., Baldo, E., Saavedra, J., Galindo, C., Fanning, C.M., 1998b. The Pampean Orogeny of the southern proto-Andes: Cambrian continental collision in the Sierras de Córdoba. In:

Pankhurst, R.J., Rapela, C.W. (Eds.), The Proto-Andean Margin of Gondwana. Geological Society of London, Special Publications 142, pp. 181–217.

Rapela, C.W., Coira, B., Toselli, A., Llambías, E.J., 1999. Sistema Famatiniano de las Sierras Pampeanas y Magmatismo eopaleozoico de las Sierras Pampeanas, de la Cordillera Oriental y Puna. In: Caminos, R. (Ed.), Geología Argentina Segemar, Anales 29, pp. 145–158.

Rochette, P., 1987. Magnetic susceptibility of the rocks matrix related to magmatic fabric studies. Journal of Structural Geology 9, 1015–1020.

Rochette, P., Jackson, M., Aubourg, C., 1992. Rock magnetism and the interpretation of anisotropy of magnetic susceptibility. Review of Geophysics 30, 209–226.

Sato, A.M., González, P.D., Llambías, E.J., 2003. Evolución del orógeno Famatiniano en la Sierra de San Luis: magmatismo de arco, deformación y metamorfismo de bajo a algo grado. Revista de la Asociación Geológica Argentina 58, 487–504.

Simpson, C., Wintsch, R.P., 1989. Evidence for deformation-induced K-feldspar replacement by myrmekite. Journal of Metamorphic Geology 7, 261–275.

Simpson, C., Law, R.D., Gromet, L.P., Miro, R., Northrup, C.J., 2003. Paleozoic deformation in the Sierras de Córdoba and Sierra de Las Minas, eastern Sierras Pampeanas, Argentina. Journal of South American Earth Sciences 15, 749–764.

Stephens, W.E., 1992. Spatial, compositional and rheological constraints on the origin and zoning in the Criffel pluton, Scotland. Transactions of the Royal Society of Edinburgh, Earth Science 83, 191–199.

Stuart-Smith, P.G., Camacho, A., Sims, J.P., Skirrow, R.G., Lyons, P., Pieters, P.E., Black, L.P., Miró, R., 1999. Uranium–lead dating of felsic magmatic cycles in the southern Sierras Pampeanas, Argentina: implications for the tectonic development of the proto-Andean Gondwana margin. In: Ramos, V.A., Keppie, J.D. (Eds.), Laurentia–Gondwana Connections before Pangea. Geological Society of America, Special Paper 336, pp. 87–114.

Trindade, R.I., Bouchez, J.L., Bolle, O., Nédélec, A.P., Poitrasson, F., 2001. Secondary fabrics revealed by remanence anisotropy: methodological study and examples from plutonic rocks. Geophysical Journal Interior 147, 310–318.

Vigneresse, J.L., 1990. Use and misuse of geophysical data to determine the shape at depth of granitic intrusions. Geological Journal 25, 249–260.

Weinberg, R.F., Sial, A.N., Mariano, G., 2004. Close spatial relationship between plutons and shear zones. Geology 32, 377–380.

Whitmeyer, S.J., Simpson, C., 2003. High strain-rate deformation fabrics characterize a kilometer-thick Paleozoic fault zone in the eastern Sierras Pampeanas, Central Argentina. Journal of Structural Geology 25, 909–922.